Infection, Genetics and Evolution 72 (2019) 86–92

Contents lists available at ScienceDirect

Infection, Genetics and Evolution

journal homepage: www.elsevier.com/locate/meegid

Research paper

The dynamic region of the peptidoglycan synthase gene, *Rv0050*, induces the growth rate and morphologic heterogeneity in *Mycobacteria*

Beilan Gao[a,1], Jie Wang[a,1], Jing Huang[b], Xiaochen Huang[a], Wei Sha[a,*], Lianhua Qin[a,*]

[a] Shanghai Key Laboratory of Tuberculosis, Clinic and Research Center of Tuberculosis, Shanghai Pulmonary Hospital, Tongji University School of Medicine, Shanghai, China

[b] Key Laboratory of Environmental Pollution Monitoring and Disease Control, Ministry of Education, Guizhou Medical University, Guiyang, Guizhou, China

ARTICLE INFO

Keywords:
Mycobacteria
Proline repeats
Bifunctional penicillin-binding protein
Phenotypic change

ABSTRACT

Mycobacterium tuberculosis (MTB) infections rely on continued growth and division. Despite the substantial global burden of tuberculosis, the underlying mechanism governing growth is incompletely understood. Bifunctional penicillin-binding protein (PBP1), encoded by Rv0050 (ponA1) of MTB, is a key peptidoglycan synthase and plays a central role in mycobacterial growth and division by its interaction with Rpf-interacting protein A (RipA, peptidoglycan endopeptidase). Our previous work suggested that the hyper-variable proline repeats are located at the N end of PBP1. In this study, we prove that altered secondary structure resulting from polymorphic proline repeats modulates the interaction between PBP1 and RipA. Without proper coordination of peptidoglycan synthase and hydrolase, cell elongation and division is also altered resulting in phenotypic changes in the population as indicated by altered dispersion, slowed growth, or shortened cell length. Together, our data reveal that polymorphisms in Rv0050 induce mycobacterial growth and morphologic changes, and hence are responsible for giving bacteria their shape.

1. Introduction

Tuberculosis (TB), caused by *Mycobacterium tuberculosis* (MTB), remains a significant global health problem (World Health Organization, 2016). It causes ill health among millions of people each year. Bacterial infections rely on continued bacterial growth and division. Despite the substantial global burden of TB, the underlying mechanism governing growth is incompletely understood.

Growth in mycobacteria is governed by cell elongation and division, which is mainly dependent upon the synthesis of new cell wall (Kieser and Rubin, 2014; Hett et al., 2008). Peptidoglycan (PG) is a major component of cell-wall architecture and is responsible for giving bacteria their shape and structural integrity (Kieser and Rubin, 2014; Hett et al., 2008; Reed et al., 2012; Cameron et al., 2015). PG formation occurs by undergoing synthesis and hydrolysis in cell cycles promoting cell elongation and division (Reed et al., 2012; Cameron et al., 2015). Bifunctional penicillin-binding protein (PBP1), encoded by the Rv0050 gene (ponA1) of MTB, is a key PG synthase. PBP1 plays a central role in cell elongation and division by its interaction with Rpf-interacting protein A (RipA, encoded by Rv1477, PG endopeptidase) (Hett et al., 2010; Chao et al., 2013). PBP1 localizes to the cell poles and septa, the sites of PG synthesis in mycobacteria (Hett et al., 2010). Its depletion results in impaired growth and misshapen cells by blocking normal cell division (Hett et al., 2010; Chao et al., 2013; Kieser et al., 2015).

Our previous work suggested that a hyper-variable trinucleotide microsatellite locus (MML0050) was located at the 3′ end of Rv0050 (Qin et al., 2011). These repeating sequences are transcribed into a repeating series of prolines. Compared to MTB reference strain H37Rv, with 7 repeats of the proline motif (m), clinical strains showed a fixed mutation of proline to serine in the last repeat motif. Sequence analysis indicated the presence of 5 alleles carrying 5–9 proline repeats and a fixed mutation of proline to serine (6–10 m) in MTB clinical strains. Amino acids repeats have been proven to trigger predictable changes in protein action (Simon and Hancock, 2009; Pelassa and Fiumara, 2015; Chavali et al., 2017) and may offer adaptive benefits for organisms (Björklund et al., 2006; Mendes et al., 2013; Toro Acevedo et al., 2017). It has been unclear whether repeating sequences of amino acids in Rv0050 protein play a role in the adaptation and vitality of MTB strains.

W-Beijing MTB strains, isolated from the Beijing area at 1995, have undergone wide global dispersion (Kremer et al., 2004; von Groll et al.,

* Corresponding authors at: Shanghai Key Laboratory of Tuberculosis, Clinic and Research Center of Tuberculosis, Shanghai Pulmonary Hospital, Tongji University School of Medicine, 507 Zhengmin Road, Shanghai 200433, China.
E-mail addresses: shfksw@126.com (W. Sha), lianhuaq1013@163.com (L. Qin).
[1] Contributed equally to this article.

https://doi.org/10.1016/j.meegid.2018.12.012
Received 10 September 2018; Received in revised form 30 November 2018; Accepted 7 December 2018
Available online 10 December 2018
1567-1348/

2010; Bifani et al., 2002). Our previous study demonstrated that nearly all samples in the W-Beijing MTB group harbored the allele with the highest number of repeats (10 m) in the MML0050 loci (Qin et al., 2011). This implied that these repeating sequences might play a role in the epidemiology of W-Beijing MTB strains.

PonA1 from *Mycobacterium* smegmatis (MSM) with high sequence similarity to Rv0050 also plays a critical role in cell growth of mycobacteria. The homologous gene (MSMEG_3145) of RipA, PBP1-interacting protein, is also present in MSM and shows high conservation with RipA (77%). MSM has been used as a model to define the function of PBP1 encoded by Rv0050 in previous studies (Hett et al., 2010; Chao et al., 2013; Kieser et al., 2015). In this study, we also have constructed a MSM mutant lacking ponA1 as a convenient tool to define the role of variation from Rv0050 in mycobacterial growth and division.

2. Material and methods

2.1. Bacterial strains and culture conditions

MSM mc^{2}155,MTB reference strain H37Rv, and 5 MTB clinical strains with different alleles of the MML0050 locus in the Rv0050 gene were grown in Sauton culture medium supplemented with 0.5 g/L KH_2PO_4, 0.5 g/L $MgSO_4.7H_2O$, 2 g/L citric acid, 0.05 g/L ferric ammonium citrate, 4.0 g/L L-asparagine, 6% glycerol, and 0.02% Tween 80.

2.2. Extraction of bacterial DNA

Strains were sterilized at 80 °C for 30 min, then collected by centrifugation (12,000 *g* for 5 min). The bacterial pellets were washed three times with sterilized saline and re-collected by centrifugation (12,000 *g* for 10 min each time). The bacterial pellets were resuspended in 50 mL DNA lysis buffer comprised of 10 mmol/L NaCl, 1 mg/mL SDS, 15% Chelex-100, and 1% Tween 20. The mixture was incubated at 50 °C for 1 h, followed by 100 °C for 10 min, then centrifuged (5000 *g* for 10 min) to obtain the aqueous phase containing genomic DNA.

2.3. Prediction of secondary structure from amino acid sequence located in proline-rich regions

The secondary structures resulting from repeated amino acid sequences located in the proline-rich region were determined by graphic analysis using the Protean module provided by DNA Star Protein software (DNA star Inc.) (Chou and Fasman, 1978a, 1978b).

2.4. Purification of PBP1 proteins with different alleles

Rv0050 genes with different alleles were amplified and cloned into the pET-28a expression plasmid, and verified by sequencing. All confirmed plasmids were transformed individually into *E. coli* BL21, and recombinant strains were grown in Luria-Bertani (LB) medium containing 100 μg/mL ampicillin at 37 °C. Isopropyl β-D-1-thiogalactopyranoside (IPTG) was added to the culture at a final concentration of 0.1 mmol/L when the absorbance at 600 nm reached 0.6–0.8. The culture was continuously incubated for 16 h at 18 °C. Afterwards, cells were harvested by centrifugation, and stored at −80 °C. Thawed bacteria were resuspended in lysis buffer (50 mmol/L Tris–HCl, 0.5 M NaCl, pH 8.0) and broken by sonication. Insoluble material was removed by centrifugation for 30 min at 19,000 × g. The soluble extract was purified by Ni2+ affinity chromatography (Qiagen, Hilden Germany) following the manufacturer's instructions. Protein purity was monitored by 12% sodium dodecyl sulfate (SDS)–polyacrylamide gel electrophoresis (PAGE) and Coomassie blue staining. The concentration was determined using a BCA protein assay kit (Thermo Fisher Scientific) with BSA as a standard.

2.5. Binding analysis of PBP1 and RipA

Purified PBP1 proteins with different alleles were used to analyze the binding between PBP1 with RipA using a ForteBio's Octet platform. The C-terminal 25 amino acids from RipA, previously proven to be the region that interacts with PBP1, were synthesized as a 25-aa peptide with the following sequence: VGLKVRVAPVRTAGMTPYVVRYIEY, and biotin-labeled at the N terminal. A streptavidin-labeled biosensor was first equilibrated incubated in PBS buffer for 30 s, then loaded with the biotin-labeled peptide (0.5 g/L) in PBS for 3 min. Next, biosensors with the biotin-labeled peptides were incubated with purified PonA1 protein in PBS (1 g/L) for 5 min to allow association; then, the labeled peptides were incubated in fresh PBS buffer for 5 min for dissociation of non-specifically bound molecules. The binding of PonA1 to RipA was analyzed with subtracted data (obtained by subtracting background data from raw data) using Octet data analysis software.

2.6. Deletion of ponA1 in MSM mc^{2}155

The ponA1-null mutant was generated by the phage transduction method (Bardarov et al., 2002). To construct a transducing phage for ponA1 knockout in the MSM mc^{2}155 strain, the left arm homologue was amplified by PCR using primers KOP1: 5′-AAGCAGAGCTCGGTGA TGTGCC-3′ and KOP2: 5′-GATCGCAGAACCGCGTCGCACCCA-3′. The right arm homologue was amplified by PCR using primers KOP3: 5′-TGACCGTGATCCAGCCGACC-3′ and KOP4: 5′-GTACTGGTAGATGC CGGTGATGA-3′. The PCR products were ligated into the *Afl*II/*Xba*I and *Hind*III/*Bgl*II sites of pYUB854. The recombinant transducing phage was used to construct the ponA1-null mutant as described. Cells were plated on 7H10 plates containing 75 μg/mL hygromycin. After incubation at 37 °C for 3–4 days, colonies were inoculated into 1 mL of selective 7H9 broth. The mutant was verified by PCR (P1: 5′- CGCGTACGGCCAGTG AATAA and P2: 5′–GTACTGGTAGATGCCGGTG-3′) and reverse transcription-PCR (P3: 5′- TTCCAGCAGAACCAGACGAC-3′ and P4: 5′-CGTAGTACGCCTTGATGCCT-3′). The relative transcriptional level was determined by agarose gel electrophoresis analysis or a $2^{-\Delta\Delta Ct}$ method. The reference gene used was 16S rRNA.

2.7. Recombinant DNA constructs

To generate different recombined ponA1 strains, alleles of ponA1 from *M. smegmatis* (MSMEG_6900), *M. tuberculosis* H37Rv, or clinical strains with different alleles were generated by PCR, and subcloned into the pvv16 plasmid. Recombinant plasmids were verified by sequencing with the universal primers for pvv16 plasmid. All confirmed plasmids were electrically transformed into *M. smegmatis*. Cells were plated on 7H10 plates containing 75 μg/mL hygromycin. After incubation at 37 °C for 5–10 days, colonies were inoculated into 1 mL of selective 7H9 broth.

2.8. Morphological observation

MSM and selected recombinant strains were grown in static Middlebrook 7H9 liquid culture to log phase at 37 °C (about 3–5 days),then 10 μl of culture were spread onto a glass slide. Smears on glass slides were fixed under the ultraviolet light overnight. Glass slides were stained with Ziehl–Neelsen stain using a TB Stain Kit (Baso DIAGNOTICS TAIWAN, Zhuhai, China). Morphological characteristics or cell lengths of tested strains were observed using a Leica DM2500 microscope using the 100× objective. Length was measured from cell pole to the opposite cell pole or from cell pole to septum(flex point), if present (Kieser et al., 2015).

2.9. In vitro growth assays

Tested strains were grown to mid-log phase in 7H9 broth with 10%

ADC, 0.05% Tween 80 and antibiotics, as required. Growth curves of each strain were determined using a Bioscreen C Growth Curve 221 Instrument (Labsystems Oy, Helsinki, Finland) and a honeycomb plate with 100 wells (Labsystems Oy). Briefly, 200 μL of each bacterial suspension, adjusted to a similar density, was added to each well and cultured with shaking at 37 °C. The optical density was measured as an absorbance at 600 nm every 2 h. Hypoxic conditions were established by covering each culture with 50 μL of paraffin oil (Liu et al., 2016; Yang et al., 2018). Cultures were incubated at 37 °C for 5 days. Two independent experiments were performed, each in triplicate. Error bars indicate the means ± SD. Two-tailed unpaired *t*-tests were used to analyze the difference of growth rate between recombinant *M. smegmatis* strains. Statistical significance was defined as $P < 0.05$.

3. Results

3.1. Variation in Rv0050 changes the intensity of interaction between PBP1 and RipA

Numerous studies have demonstrated that certain amino acids repeat motifs can mediate protein-protein interactions by forming super-secondary structures(Pelassa and Fiumara, 2015; Pelassa et al., 2014; Schaefer et al., 2012). Proline-rich sequences have been reported to mediate protein-protein interactions by binding to non-repetitive interaction domains (Schaefer et al., 2012; Yu et al., 1994). The C-terminal 150 amino acids of Rv0050, including the proline-rich region, proved to be important for the interaction of PBP1 with RipA (Hett et al., 2010). Thus, we hypothesized that it is very possible that the variations in the proline repeats located in the 54 amino acid proline-rich region of PBP1 (Fig. 1) may regulate the interaction of PBP1 with RipA by inducing changes in the secondary structure of PBP1 and its binding to RipA. To test this hypothesis, we predicted the amino acid secondary structure of proline-repeat sequences located in the proline-rich region. Variations in the repeated sequences did change the amino acid secondary structure, primarily in the turn regions, coil regions, α- or β-amphipathic regions, and flexible region (Fig. 2a). The flexible region and the α-amphipathic regions displayed prominent differences in secondary structure in 5 alleles (6 m–10 m). To determine the role of secondary-structure differences in the 5 alleles in the interaction between PBP1 and RipA, we analyzed the intensity of interaction between RipA and various alleles of PBP1 (Fig. 2b). Processed kinetic data showed that the expansion of proline repeats decreased the intensity of the interaction between PBP1 and RipA (Fig. 2b). Among the 5 alleles, $Rv0050_{6m}$ exhibited the highest affinity for RipA while $Rv0050_{10m}$ exhibited the lowest affinity for RipA. Variations of the proline-rich region of Rv0050 regulated the intensity of the interaction between PBP1 and RipA.

3.2. PonA1 is required for normal growth and cell division in mycobacteria

The interaction between PBP1 and RipA was previously confirmed to have an important role in mycobacterial growth and the formation of abnormal cell shape (Hett et al., 2010). To define the role of variation in the Rv0050 gene in bacterial phenotype and growth, a MSM mutant lacking ponA1 (△ponA1), a highly homologous gene of Rv0050, was constructed as a convenient tool (Fig. 3). The deletion of ponA1 severely impacted proliferation of MSM, which displayed a low growth rate, shortened cell length, and induced the formation of ballooning cells (Figs. 4,5), as previously reported (Hett et al., 2010).

The overexpression of wildtype Rv0050 from the MTB reference strain H37Rv (△ponA1:: $Rv0050_{wt,}$ including seven intact perfect proline-motifs in the MML0050 locus) or wildtype ponA1 from MSM (△ponA1:: ponA1) in △ponA1 MSM cells both restored the mutant to normal growth and returned the bacteria to a typical morphology (Figs. 4,5). Nevertheless, the △ponA1::$Rv0050_{wt}$ complementation strain displayed a remarkably high growth rate both under aerobic ($p = 0.0170$) and hypoxic conditions ($p = 0.0013$), compared with the complementation strains containing wildtype ponA1 from MSM. These data suggest that ponA1 is required for normal growth and cell division in mycobacteria.

Moreover, we found that a single mutation in the proline-rich region (the fixed mutation of proline to serine in MTB clinical strains) was not responsible for the remarkable difference in cell length and growth rate between △ponA1:: $Rv0050_{wt}$ with seven perfect proline motifs and △ponA1:: $Rv0050_{7m}$ with a mutation of proline to serine in the seventh repeat motif ($p > 0.05$). As we previously reported, the mutation in the last repeat motif of the MML0050 locus simply confined the expansion or contraction of repeat sequences to avoid the formation of conspicuously long simple sequence repeats in MTB clinical strains (Qin et al., 2011), but did not influence the growth rate or cell division differences observed between the wildtype ($Rv0050_{wt}$) and the mutant ($Rv0050_{7m}$).

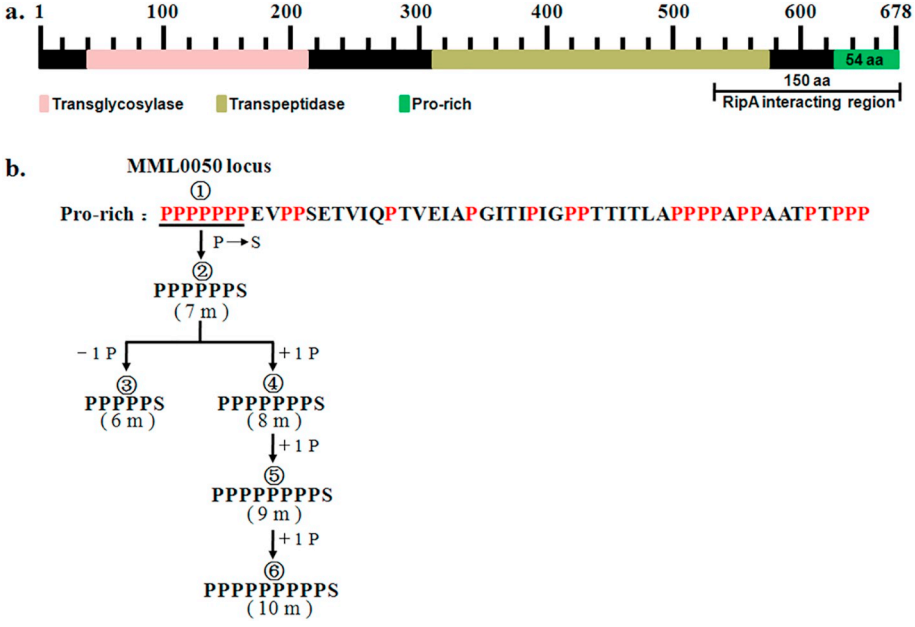

Fig. 1. Diagram depicting Rv0050 a. Organization of the Rv0050 protein (a bifunctional peptidoglycan synthase) containing a transglycosylase domain at the N-terminus,a transpeptidase domain, and a 54 aa (amino-acid) proline-rich region at the C-terminus. The C-terminal 150 aa, including the proline-rich region, comprise the region responsible for interaction with RipA. b. Variations of amino-acid sequences from the proline-rich region are located in the RipA interacting region.

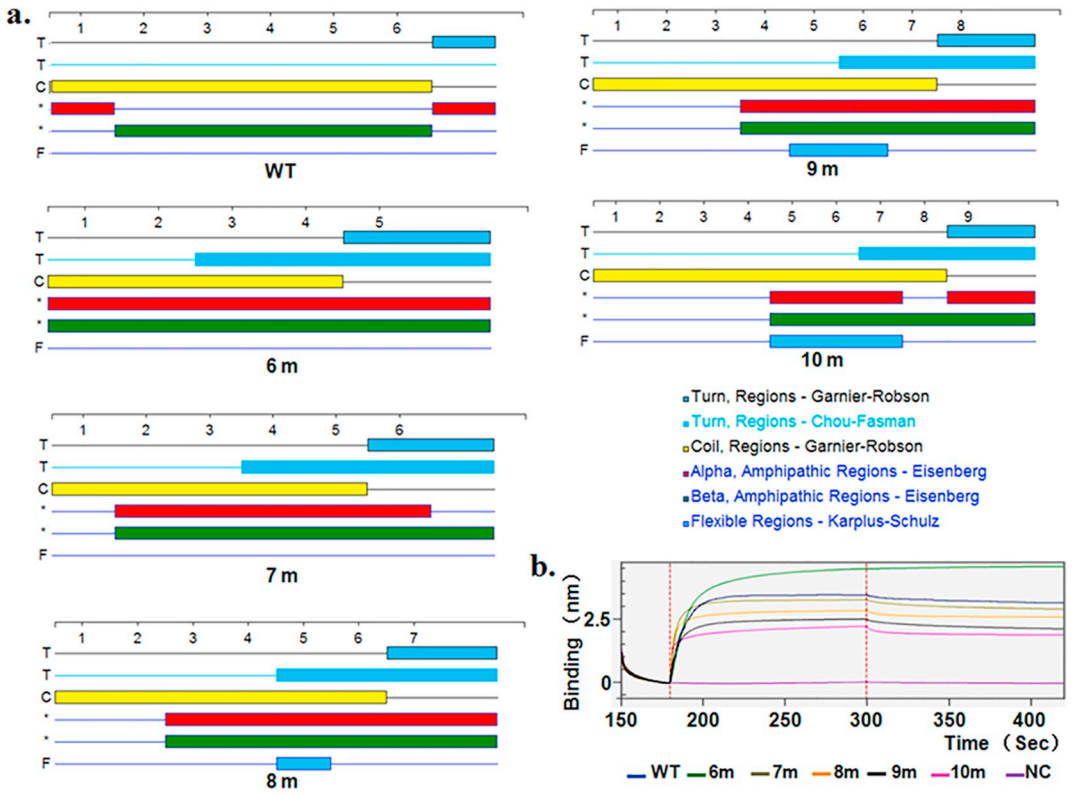

Fig. 2. Variable binding of different alleles of Rv0050 to RipA. a. Prediction of secondary structure of the repeat motif sequences determined by graphic analysis using the Protean module provided by DNA Star Protein software (DNAstar Inc.). Variations in the region containing repeated sequences resulted in alterations in amino-acid secondary structure, primarily in the turn regions, coil regions, α- or β-amphipathic regions, and the flexible region. b. Processed kinetic data for different alleles of the Rv0050 gene product and the PBP1-binding domain (25 amino-acids) of RipA by a ForteBio's Octet platform. The 6 m allele exhibited the highest affinity for RipA while the 10 m allele exhibited the lowest affinity for RipA. WT: wildtype from MTB reference strain H37Rv; NC: Negative control.

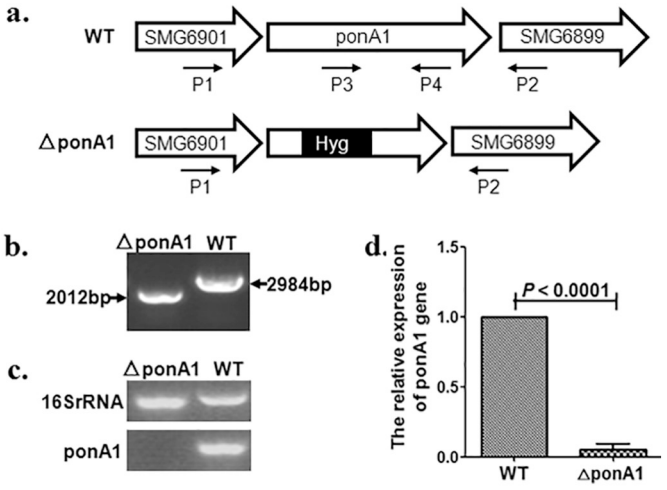

Fig. 3. Generation of ponA1 depletion strains a. Schematic diagrams of wild-type (WT) and the ponA1-null (△ponA1) mutant. The mutant was verified by PCR (P1 and P2) and reverse transcription-PCR (P3 and P4). The primers used for PCR are shown as arrows. b. Agarose gel electrophoresis analysis of the PCR amplification product from WT strain or △ponA1 using primers P1 and P2. c. mRNA from WT strain or △ponA1 were reverse transcribed, followed by PCR amplification using primers P3 and P4, and then subjected to agarose gel electrophoresis analysis. d. The relative transcriptional level was determined by a $2^{-\Delta\Delta Ct}$ method. The expression of tested genes was normalized to that of 16S rRNA. Values represent the mean ± SD from three independent experiments. Student's *t*-test.

3.3. Variation in Rv0050 regulates bacterial shape and growth

The morphological characteristics of △ponA1 MSM cells over-expressing different alleles of Rv0050 (6 m to 10 m) were observed (△ponA1:: $Rv0050_{6m–10m}$). We found that △ponA1:: $Rv0050_{7m–9m}$ exhibited normal cell length and chrysanthemum shapes as compared to the control groups including wild MSM, △ponA1::ponA1, and △ponA1::$Rv0050_{wt}$ (Figs. 4,5). However, △ponA1::$Rv0050_{6m}$ cells tended to exhibit more dispersion in growth and did not display cluster growth, yet there were no significant changes in individual cellular length. By contrast, △ponA1::$Rv0050_{10m}$ cells exhibited shortened cell length, but normal cell shape as compared to the control groups. Taken together, these data show that variation in the Rv0050 gene governs bacterial length and shape.

Growth rates of △ponA1 MSM cells expressing different alleles of MTB Rv0050 were also tested under aerobic or hypoxic conditions. We found that the 5 alleles ($Rv0050_{6m–10m}$) all complemented the cell growth of △ponA1 MSM under both aerobic and hypoxic growth conditions ($p < 0.05$). Under aerobic conditions, each of the 5 alleles failed to induce significant differences in growth rate ($p > 0.05$). Under hypoxic growth conditions, △ponA1::$Rv0050_{6m}$ exhibited growth dispersion while△ponA1:: $Rv0050_{10m}$ cells exhibited shortened cell length but normal cell shape along with a significantly lower growth rate ($p < 0.05$) as compared with △ponA1:: $Rv0050_{7m–9m}$. The △ponA1::$Rv0050_{7m–9m}$ alleles displayed normal cell length and cellular morphology along with a similar growth rate under hypoxic conditions ($p > 0.05$). In this study, we found that variation in Rv0050 regulated bacterial growth under hypoxic conditions.

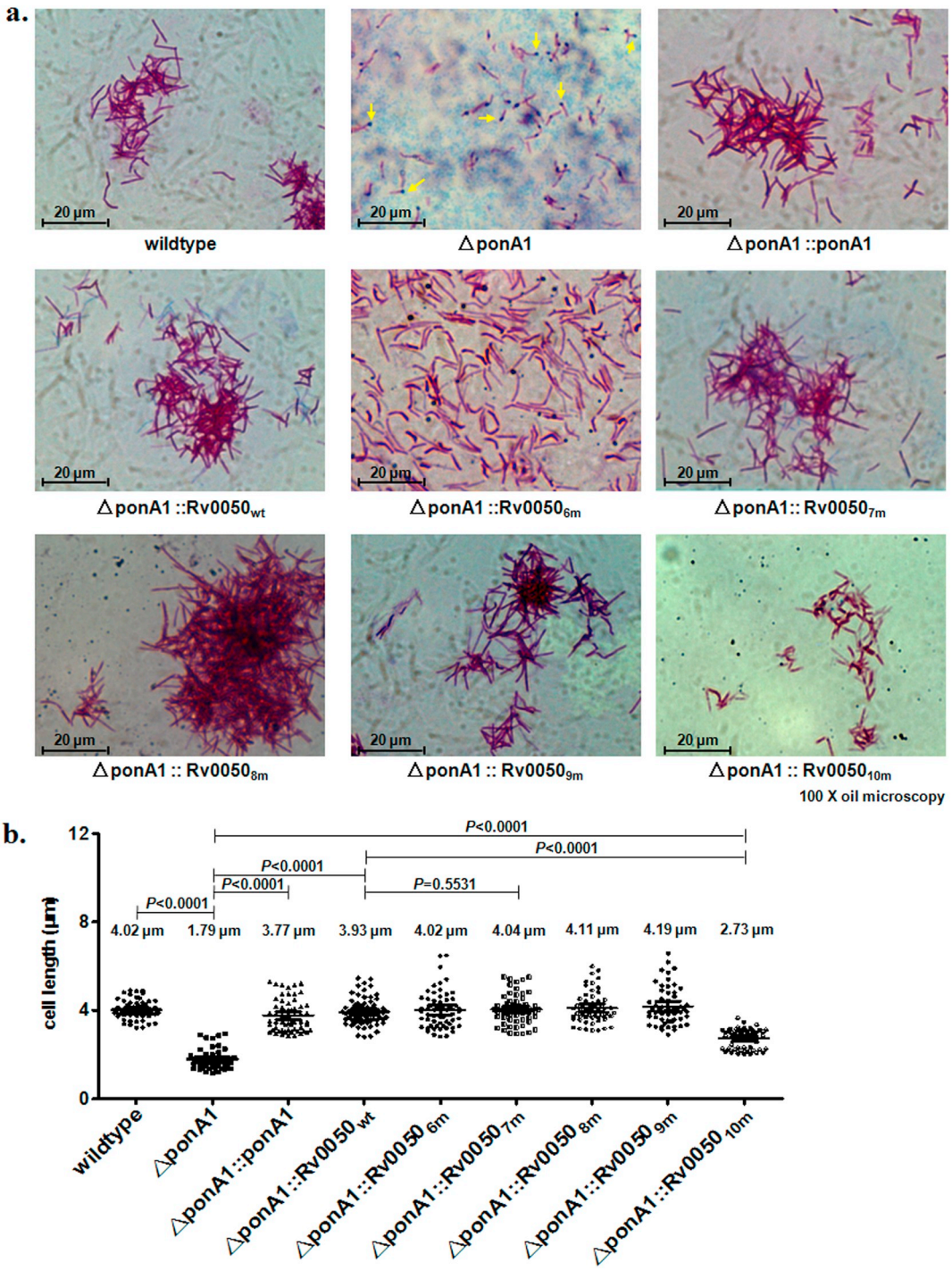

Fig. 4. Rv0050 controls normal bacterial shape in mycobacteria.
Wildtype, △ponA1, and △ponA1 MSM cells overexpressing ponA1 from MSM (△ponA1::ponA1), wildtype Rv0050 from the MTB reference strain H37Rv (△ponA1:: $Rv0050_{wt}$, including intact seven perfect Pro-motifs in MML0050 locus) or different alleles of Rv0050 (6 m to 10 m; △ponA1:: $Rv0050_{6m–10m}$) from the MTB clinical strains were analyzed for bacterial shape (a), cell length (b) by a Leica DM2500 microscope using the 100× objective. Length was measured from cell pole to the opposite cell pole or from cell pole to septum(flex point), if present. Total cell length was measured: Wildtype (65 cells), △ponA1 (51 cells),△ponA1::ponA1 (61 cells), △ponA1:: $Rv0050_{wt}$ (71 cells), △ponA1:: $Rv0050_{6m}$ (61 cells), △ponA1:: $Rv0050_{7m}$ (63 cells), △ponA1:: $Rv0050_{8m}$ (56 cells), △ponA1:: $Rv0050_{9m}$ (56 cells), △ponA1:: $Rv0050_{10m}$ (55 cells). Depletion of ponA1 blocks normal bacterial shape and induces the formation of ballooning cells (indicated by yellow arrows). △ponA1:: $Rv0050_{7m–9m}$ exhibited normal cell length and chrysanthemum shapes. △ponA1::$Rv0050_{6m}$ cells tended toward more dispersive growth and did not display characteristic cluster growth while there were no significant differences in cell length. By contrast, △ponA1::$Rv0050_{10m}$ cells exhibited shortened cell length, but normal cell shape as compared to other alleles. (For interpretation of the references to colour in this figure legend, the reader is referred to the web version of this article.)

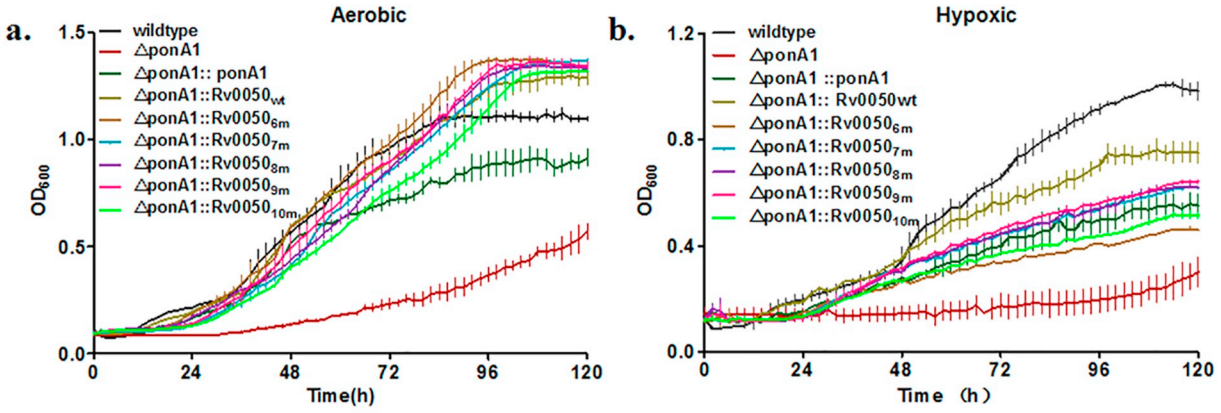

Group	P value
wildtype vs ΔponA1:	p<0.0001
ΔponA1 vs ΔponA1::ΔponA1	p<0.0001
ΔponA1 vs ΔponA1::$Rv0050_{wt}$	p<0.0001
ΔponA1::ΔponA1 vs ΔponA1::$Rv0050_{wt}$	p=0.0170
ΔponA1::$Rv0050_{wt}$ vs ΔponA1::$Rv0050_{7m}$	p=0.7835
ΔponA1::$Rv0050_{10m}$ vs ΔponA1::$Rv0050_{6m}$	p=0.1233
ΔponA1::$Rv0050_{10m}$ vs ΔponA1::$Rv0050_{7m}$	p=0.5308
ΔponA1::$Rv0050_{10m}$ vs ΔponA1::$Rv0050_{8m}$	p=0.4483
ΔponA1::$Rv0050_{10m}$ vs ΔponA1::$Rv0050_{9m}$	p=0.3286

Group	P value
wildtype vs ΔponA1	p<0.0001
ΔponA1 vs ΔponA1::ΔponA1	p<0.0001
ΔponA1 vs ΔponA1::$Rv0050_{wt}$	p<0.0001
ΔponA1::ΔponA1 vs ΔponA1::$Rv0050_{wt}$	p=0.0013
ΔponA1::$Rv0050_{wt}$ vs ΔponA1::$Rv0050_{7m}$	p=0.0566
ΔponA1::$Rv0050_{6m}$ vs ΔponA1::$Rv0050_{7m}$	p=0.0079
ΔponA1::$Rv0050_{6m}$ vs ΔponA1::$Rv0050_{8m}$	p=0.0073
ΔponA1::$Rv0050_{6m}$ vs ΔponA1::$Rv0050_{9m}$	p=0.0031
ΔponA1::$Rv0050_{6m}$ vs ΔponA1::$Rv0050_{10m}$	p=0.3904
ΔponA1::$Rv0050_{10m}$ vs ΔponA1::$Rv0050_{7m}$	p=0.0468
ΔponA1::$Rv0050_{10m}$ vs ΔponA1::$Rv0050_{8m}$	p=0.0489
ΔponA1::$Rv0050_{10m}$ vs ΔponA1::$Rv0050_{9m}$	p=0.0297

Fig. 5. Rv0050 controls bacterial growth.
Wildtype, △ponA1, and △ponA1 complementation mutants were grown to mid-log phase, and the growth curve under aerobic or hypoxic conditions were measured using a Bioscreen Growth Curve Instrument. Hypoxic conditions were established by covering bacterial suspensions with paraffin oil. The optical density was measured as an absorbance at 600 nm every 2 h. Cultures were grown at 37 °C for 5 days. Results were combined (mean ± standard deviation [SD]) from two independent experiments, with each experiment performed in triplicate. Depletion of ponA1 induces low growth rate compared with wildtype. PonA1 is required for normal growth both under aerobic and hypoxic conditions. Under hypoxic growth conditions, △ponA1::$Rv0050_{6m}$ and △ponA1::$Rv0050_{10m}$ cells displayed a significantly lower growth rate ($p < 0.05$), as compared with △ponA1:: $Rv0050_{7m–9m}$.

4. Discussion

Proteins containing repetitive amino-acid domains are widespread in all lifeforms (Marcotte et al., 1999; Faux, 2012). These regions are thought to be a major source of genetic variation, affecting both protein structure and function (Faux, 2012; Katti et al., 2000) and may offer organisms adaptive benefits in the face of selective pressure (Kedzierski et al., 2004; Ampattu et al., 2017). A growing body of evidence indicates amino acid repeats regulate the function of proteins by mediating interactions with other proteins via the formation of super-secondary structures (Björklund et al., 2006; Fiumara et al., 2010). Similar mechanisms also exist in mycobacteria. HBHA (heparin-binding haemagglutinin) mediates the adhesion of MTB to epithelial cells via the interaction of its C-terminal lysine-rich repeat domain with sulfated glycoconjugates on the surface of epithelial cells (Lebrun et al., 2012). The C-terminal low-complexity sequence repeats of *M. smegmatis* Ku significantly modulates DNA-binding properties and promotes DNA end-joining (Kushwaha and Grove, 2013). Our data demonstrated that proline repeats located in the Rv0050 protein mediate interactions between PBP1 and RipA, primarily by altering the flexible region and the α-amphipathic regions of its secondary structure (Fig. 2). Among the 5 alleles, $Rv0050_{10m}$ with the highest numbers of repeats, exhibited the lowest affinity for RipA, while $Rv0050_{6m}$ with the lowest numbers of repeat had the highest affinity for RipA. The intensity of interaction between PonA1 and RipA was decreased with the expansion of proline repeats. As reported, RipA not only interacts with PBP1 but also interacts with the lytic transglycosylase, RpfB. The complex of RipA and RpfB exhibits synergistic hydrolysis of PG (Hett et al., 2008; Hett et al., 2007). Moreover, RipA interacts with PBP1 at the same C terminal 25 amino acids of RipA required for RpfB binding (Hett et al., 2010). PBP1 and RpfB are competitive for binding to RipA. This competition coordinates septal PG synthesis and division and modulates cell elongation or division; it may also, subsequently, impact bacterial phenotype and growth (Hett et al., 2010).

Since the variations present in Rv0050 can regulate its interaction with RipA, it is very possible that the variations in Rv0050 may regulate PG remodeling by changing the intensity of the interaction between Rv0050 and RipA, thereby inducing both growth rate and morphology heterogeneity. When the interaction between PBP1 and RipA is intensified, cells displayed a dispersing, not normal cluster growth while its lengths did not exhibit gross differences. When the interaction between Rv0050 and RipA is weak, cells exhibited shortened cell length while displaying normal cluster growth. Given the competition between PBP1 and RpfB for binding to RipA, the intensified ($Rv0050_{6m}$) or weakened ($Rv0050_{10m}$) interaction between Rv0050 and RipA may inhibit or improve the interaction of RipA and RpfB and their synergy in PG hydrolysis. Without proper coordination of PG synthase and hydrolase, cell elongation and division may be changed and result in phenotypic heterogeneity of a population such as a dispersing growth (single cell's branching behaviors may be regressed) or shortened cell length (single cell elongation may be dampened) (Fig. 4). Moreover, the weakened interaction intensity between Rv0050 and RipA remarkably slowed the cell growth rate, especially under hypoxic growth conditions (Fig. 5).

Recent studies have shown that cell contraction (shortened cell length) facilitates bacterial resistibility to environment stress (such as drug), reduces attacks from the immune system, and increases bacterial survival (Van Teeseling et al., 2017; Rego et al., 2017; Veyrier et al.,

2015). This may give an explanation that why nearly all samples in W-Beijing MTB group with wide global dispersion harbors the allele with the highest repeat numbers (10 m) of Rv0050 (Qin et al., 2011).

5. Conclusions

Tuberculosis caused by *Mycobacterium tuberculosis*(MTB) infection remains a huge global public health problem. Bacterial infections rely on continued growth and division. More research is needed to further unravel the mechanisms underlying mycobacterial growth and division, and to examine the implications for future control strategies. Our data suggest that polymorphisms of Rv0050 alter interactions between peptidoglycan synthase and hydrolase, resulting in reduced growth rate and morphologic heterogeneity. Subsequently, these phenotypic characteristics may confer a fitness advantage to pathogenic bacteria in the face of selective pressure.

Funding

This work was supported by National Natural Science Foundation of China (81470090 and 81201254).

Conflicts of interest

The authors declare no conflicts of interest.

References

Ampattu, B.J., Hagmann, L., Liang, C., Dittrich, M., Schlüter, A., Blom, J., et al., 2017. Transcriptomic buffering of cryptic genetic variation contributes to meningococcal virulence. BMC Genomics 18 (1), 282.

Bardarov, S., Bardarov Jr., S., Pavelka Jr., M.S., Sambandamurthy, V., Larsen, M., Tufariello, J., et al., 2002. Specialized transduction: an efficient method for generating marked and unmarked targeted gene disruptions in *Mycobacterium tuberculosis, M bovis* BCG and *M. smegmatis*. Microbiology 148 (Pt 10), 3007–3017.

Bifani, P.J., Mathema, B., Kurepina, N.E., Kreiswirth, B.N., 2002. Global dissemination of the *Mycobacterium tuberculosis* W-Beijing family strains. Trends Microbiol. 10 (1), 45–52.

Björklund, A.K., Ekman, D., Elofsson, A., 2006. Expansion of protein domain repeats. PLoS Comput. Biol. 2 (8), e114.

Cameron, T.A., Zupan, J.R., Zambryski, P.C., 2015. The essential features and modes of bacterial polar growth. Trends Microbiol. 23, 347–353.

Chao, M.C., Kieser, K.J., Minami, S., Mavrici, D., Aldridge, B.B., Fortune, S.M., et al., 2013. Protein complexes and proteolytic activation of the cell wall hydrolase RipA regulate septal resolution in Mycobacteria. PLoS Pathog. 9, e1003197.

Chavali, S., Chavali, P.L., Chalancon, G., de Groot, N.S., Gemayel, R., Latysheva, N.S., et al., 2017. Constraints and consequences of the emergence of amino acid repeats in eukaryotic proteins. Nat. Struct. Mol. Biol. 24 (9), 765–777.

Chou, P.Y., Fasman, G.D., 1978a. Empirical predictions of protein conformation. Annu. Rev. Biochem. 47, 251–276.

Chou, P.Y., Fasman, G.D., 1978b. Prediction of the secondary structure of proteins from their amino acid sequence. Adv Enzymol. Relat. Areas Mol. Bid. 47, 45–148.

Faux, N., 2012. Single amino acid and trinucleotide repeats: function and evolution. Adv. Exp. Med. Biol. 769, 26–40.

Fiumara, F., Fioriti, L., Kandel, E.R., Hendrickson, W.A., 2010. Essential role of coiled coils for aggregation and activity of Q/N-rich prions and PolyQ proteins. Cell 143, 1121–1135.

Hett, E.C., Chao, M.C., Steyn, A.J., Fortune, S.M., Deng, L.L., Rubin, E.J., 2007. A partner for the resuscitation-promoting factors of *Mycobacterium tuberculosis*. Mol. Microbiol. 66 (3), 658–668 2007.

Hett, E.C., Chao, M.C., Deng, L.L., Rubin, E.J., 2008. A mycobacterial enzyme essential for cell division synergizes with resuscitation-promoting factor. PLoS Pathog. 4 (2), e1000001.

Hett, E.C., Chao, M.C., Rubin, E.J., 2010. Interaction and modulation of two antagonistic cell wall enzymes of Mycobacteria. PLoS Pathog. 6, e1001020.

Katti, M.V., Sami-Subbu, R., Ranjekar, P.K., Gupta, V.S., 2000. Amino acid repeat patterns in protein sequences: their diversity and structural-functional implications. Protein Sci. 9, 1203–1209.

Kedzierski, Ł., Montgomery, J., Curtis, J., Handman, E., 2004. Leucine-rich repeats in host-pathogen interactions. Arch. Immunol. Ther. Exp. 52, 104–112.

Kieser, K.J., Rubin, E.J., 2014. How sisters grow apart: mycobacterial growth and division. Nat. Rev. Microbiol. 12, 550–562.

Kieser, K.J., Boutte, C.C., Kester, J.C., Baer, C.E., Barczak, A.K., Meniche, X., et al., 2015. Phosphorylation of the peptidoglycan synthase pona1 governs the rate of polar elongation in Mycobacteria. PLoS Pathog. 11 (6), e1005010.

Kremer, K., Glynn, J.R., Lillebaek, T., Niemann, S., Kurepina, N.E., Kreiswirth, B.N., et al., 2004. Definition of the Beijing/W lineage of *Mycobacterium tuberculosis* on the basis of genetic markers. J. Clin. Microbiol. 42 (9), 4040–4049.

Kushwaha, A.K., Grove, A., 2013. C-terminal low-complexity sequence repeats of *Mycobacterium smegmatis* Ku modulate DNA binding. Biosci. Rep. 33 (1), 175–184.

Lebrun, P., Raze, D., Fritzinger, B., Wieruszeski, J.M., Biet, F., Dose, A., et al., 2012. Differential contribution of the repeats to heparin binding of HBHA, a major adhesin of *Mycobacterium tuberculosis*. PLoS ONE 7 (3), e32421.

Liu, Z.H., Gao, Y.L., Yang, H., Bao, H.Y., Qin, L.H., Zhu, C.T., et al., 2016. Impact of Hypoxia on Drug Resistance and Growth Characteristics of *Mycobacterium tuberculosis* Clinical Isolates. PLoS ONE 11 (11), e0166052.

Marcotte, E.M., Pellegrini, M., Yeates, T.O., Eisenberg, D., 1999. A census of protein repeats. J. Mol. Biol. 293, 151–160.

Mendes, T.A., Lobo, F.P., Rodrigues, T.S., Rodrigues-Luiz, G.F., Darocha, W.D., Fujiwara, R.T., et al., 2013. Repeat-enriched proteins are related to host cell invasion and immune evasion in parasitic protozoa. Mol. Biol. Evol. 30 (4), 951–963.

Pelassa, I., Fiumara, F., 2015. Differential occurrence of interactions and interaction domains in proteins containing homopolymeric amino acid repeats. Front. Genet. 6, 345.

Pelassa, I., Corà, D., Cesano, F., Monje, F.J., Montarolo, P.G., Fiumara, F., 2014. Association of polyalanine and polyglutamine coiled coils mediates expansion disease-related protein aggregation and dysfunction. Hum. Mol. Genet. 23, 3402–3420.

Qin, L.H., Wang, J., Zheng, R.J., Lu, J.M., Yang, H., Liu, Z.H., et al., 2011. Perspective on sequence evolution of microsatellite locus (CCG)n in Rv0050 gene from *Mycobacterium tuberculosis*. BMC Evol. Biol. 11, 247.

Reed, P., Atilano, M.L., Alves, R., Hoiczyk, E., Sher, X., Reichmann, N.T., et al., 2012. From the regulation of peptidoglycan synthesis to bacterial growth and morphology. Nat. Rev. Microbiol. 10, 123–136.

Rego, E.H., Audette, R.E., Rubin, E.J., 2017. Deletion of a mycobacterial divisome factor collapses single-cell phenotypic heterogeneity. Nature 546, 153–157.

Schaefer, M.H., Wanker, E.E., Andrade-Navarro, M.A., 2012. Evolution and function of CAG/polyglutamine repeats in protein-protein interaction networks. Nucleic Acids Res. 404, 273–287.

Simon, M., Hancock, J.M., 2009. Tandem and cryptic amino acid repeats accumulate in disordered regions of proteins. Genome Biol. 10 (6), R59.

Toro Acevedo, C.A., Valente, B.M., Burle-Caldas, G.A., Galvão-Filho, B., Santiago, H.D.C., Esteves Arantes, R.M., et al., 2017. Down modulation of host immune response by amino acid repeats present in a trypanosoma cruzi ribosomal antigen. Front. Microbiol. 8, 2188.

Van Teeseling, M.C.F., de Pedro, M.A., Cava, F., 2017. Determinants of bacterial morphology: from fundamentals to possibilities for antimicrobial targeting. Front. Microbiol. 8, 1264.

Veyrier, F.J., Biais, N., Morales, P., Belkacem, N., Guilhen, C., Ranjeva, S., et al., 2015. Common cell shape evolution of two nasopharyngeal pathogens. PLoS Genet. 11 (7), e1005338.

von Groll, A., Martin, A., Stehr, M., Singh, M., Portaels, F., da Silva, P.E., et al., 2010. Fitness of *Mycobacterium tuberculosis* strains of the W-Beijing and non-W-Beijing genotype. PLoS ONE 5 (4), e10191.

World Health Organization, 2016. Global tuberculosis report 2016. WHO/HTM/TB/2016.13.

Yang, H., Sha, W., Liu, Z.H., Tang, T.Q., Liu, H.P., Qin, L.H., et al., 2018. Lysine acetylation of DosR regulates the hypoxia response of *Mycobacterium tuberculosis*. Emerg. Microbes Infect. 7, 34.

Yu, H., Chen, J.K., Feng, S., Dalgarno, D.C., Brauer, A.W., Schreiber, S.L., 1994. Structural basis for the binding of proline-rich peptides to SH3 domains. Cell 7, 933–945.